

# Analysis of Low-Frequency Squeal in Automotive Disc Brake by Optimizing Groove and Caliper Shapes

Cheol Kim<sup>1</sup>#, Yonghwan Kwon<sup>1</sup>, and Dongwon Kim<sup>2</sup>

<sup>1</sup> Department of Mechanical Engineering, Kyungpook National University, 80, Daehak-ro, Buk-gu, Daegu, 41566, Republic of Korea

<sup>2</sup> Research & Development Division, Hyundai Motor, 150 Hyundaiyeonguso-Ro, Hwaseong-Si, Gyeonggi-Do 18280, Republic of Korea

# Corresponding Author / E-mail: kimchul@knu.ac.kr, TEL: +82-53-950-6586

ORCID: 0000-0003-1160-5585

KEYWORDS: Low frequency squeal, Complex eigenvalue analysis, Disc groove, Contribution factor, Disc vibration

*A low-frequency squeal that occurs due to the coupling phenomena of various vibrational modes in a disc brake system may cause annoyance to passengers. In an effort to remove the irritating low-frequency squeal of the disc brake, we carried out complex eigenvalue analysis and investigated the contribution ratio of each part to the occurrence of squealing. To this end, we developed a reliable and accurate finite element (FE) model of each brake part and compared it to the model test results. Throughout the complex eigenvalue analysis for the FE models, all unstable modes and corresponding frequencies in the brake system were calculated. The dominant parts that contributed largely to the squealing of the brake system were also elicited by the component contribution factor (CCF) analysis. Parts such as the disc, carrier, pad, and knuckle, were determined as large contributors to squealing. To reduce squealing, the tie-bar shape and the groove shape around the disc hub were optimized by FE-based shape optimization. A new disc with an optimal groove and a new tie-bar were manufactured, and dynamo squeal tests were conducted for a comparison to the numerical prediction. A fairly good correlation was observed between the experimental and numerical analysis results.*

Manuscript received: March 30, 2017 / Revised: June 8, 2017 / Accepted: January 8, 2018

## 1. Introduction

The fundamental mechanism involved in the onset of a disc brake squeal is the coupling phenomena of various vibrational modes in the disc brake system. Squealing may compromise the comfort of passengers. The instantaneous change of normal contacting forces between the disc and pads is caused by the vibrational mode coupling of the disc and supplies energy for squealing. A great deal of effort has been put into reducing the brake squeal noise of cars. As the result of the first analytic study on disc squealing, squealing was identified as a self-excited vibration induced by friction forces.<sup>1</sup> Since then, a large number of squeal analyses have been carried out by various minimal models that were constructed with a disc and pads, in order to identify the fundamental characteristics of disc squeal.<sup>2-11</sup> Even though the minimal model had some advantages, it could not accurately predict the occurrence of squeal.

Instead of the usual lumped parameter model, various detailed finite element (FE) disc brake models with a disc, two pads, lining material, caliper, etc., were constructed and analyzed. Complex eigenvalue analysis (CEA) was performed in order to solve the equations of

motion of the system.<sup>2,12,13</sup> The disc and mounting bracket have been reported to exert strong influence on brake squeal. Researchers who investigated a comprehensive FE model of the rotating disc brake reported that the occurrence of squeal was affected by the mode-coupling, gyroscopic effect, and negative slope effect.<sup>14-17</sup> However, a change in design that may effectively suppress the squealing has not been suggested in previous studies. Recently, an improved friction-coupled analysis method was suggested, considering the damping of the pad lining material by using the finite element method (FEM) and the equations of motion.<sup>18</sup> Lee (2000) attempted to optimize the complex eigenvalues of brake components.<sup>19</sup> Previous experimental and analytical studies on disc brake squealing have been reviewed by Mohammed and Rahim (2013).<sup>20</sup> Since complex eigenvalue analysis was applied to the lumped model of a disc brake,<sup>21</sup> many studies on the occurrence of squeal in complicated brake systems with many components have been conducted by using the FEM.<sup>22-26</sup> In addition, the thermo-mechanical behavior at the dry contact between disc and pad during braking was analyzed by FEM.<sup>27-30</sup> In most of the previous studies on this subject, the stiffness of the car frame had not been considered in any way, and important disc brake housing parts and components, such as the housing,

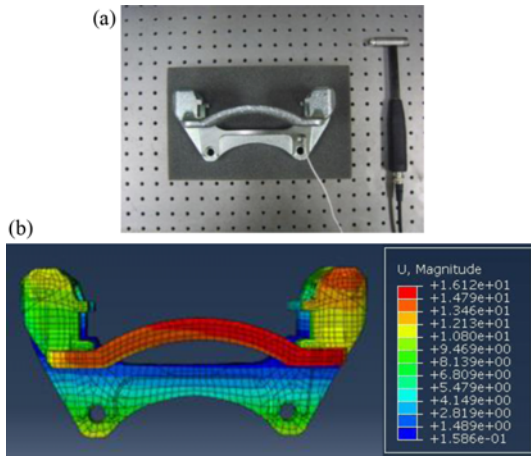


Fig. 1 Actual (a) and finite element carriers (b) of disc brake caliper (legend: amplitude [mm])

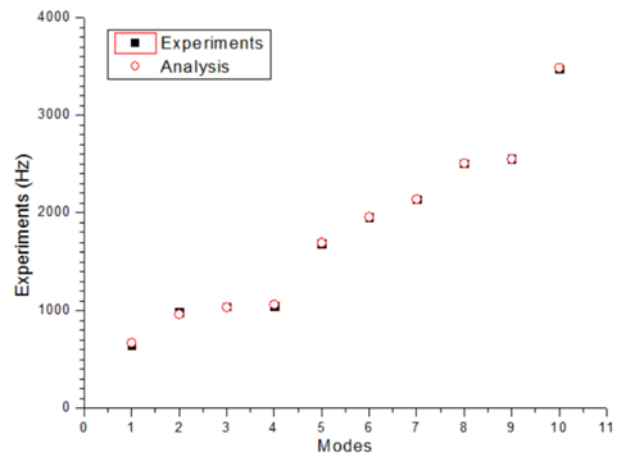


Fig. 2 Natural frequencies obtained from modal tests and finite element analysis of carrier

piston and an oil seal, knuckle and its bearings, pad springs, carrier, and guide rod, which have a strong influence on squealing, had not been included in the investigated FEM models. Suggestions were not made for realistic and specific design changes for the purpose of reducing squealing, and the experimental validation of new design ideas produced by numerical studies is also sparse in the literature. Brake noise can be categorized in three groups, depending on the frequency range, namely low-frequency noise (0-1 kHz), low-frequency squeal (1-3 kHz), and high-frequency squeal (3-15 kHz) (Dai and Lim, 2008).<sup>26</sup> The goal of this study is to remove the low-frequency squeal of a targeted disc brake system by modifying the disc that has a strong influence on the occurrence of the low-frequency squeal. To do so, we develop an accurate FE model of the caliper disc brake system, including all the caliper parts and knuckle. The shape of the optimal undercut around the disc hub is created by adjusting the disc stiffness through the implementation of FE-based shape optimization. Moreover, complex eigenvalue analysis is carried out and a modified disc with an optimal under-cut is manufactured and tested in order to prove the accuracy of FEM optimization.

**2. Modal Tests and FE Modeling**

Modal tests were conducted (Figs. 1(a), 3(a), and 5(a)), and the test results were compared to numerical ones in order to validate the accuracy of each FE model used in vibration analysis. 3-D FE analysis models for the parts comprising a disc brake system of a passenger car were also constructed as shown in Figs. 1(b), 3(b), and 5(b). Subsequently, their natural frequencies were computed. The numerical and experimental natural frequencies were plotted together in Figs. 2, 4, and 6, and show a good correlation. Additionally, experimental (Fig. 7(a)) and numerical frequencies (Fig. 7(b)) from the assembly of the disc, a knuckle, and a carrier were also compared and a discrepancy of 1.83% was observed between the two results.

The finite element model of the brake system, which consists of full parts including the knuckle, disc, caliper, carrier, and others, was assembled, as shown in Fig. 8, in order to accurately predict the

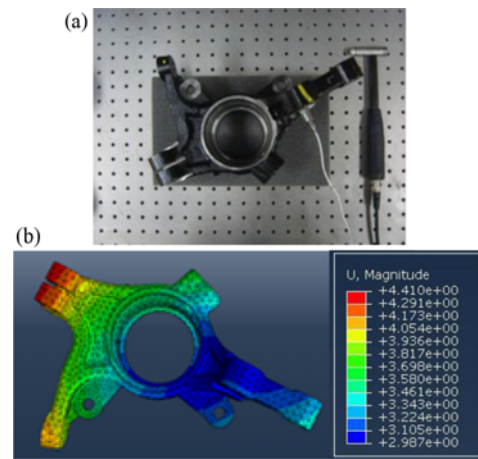


Fig. 3 Actual (a) and finite element knuckles (b) of disc brake (legend: amplitude [mm])

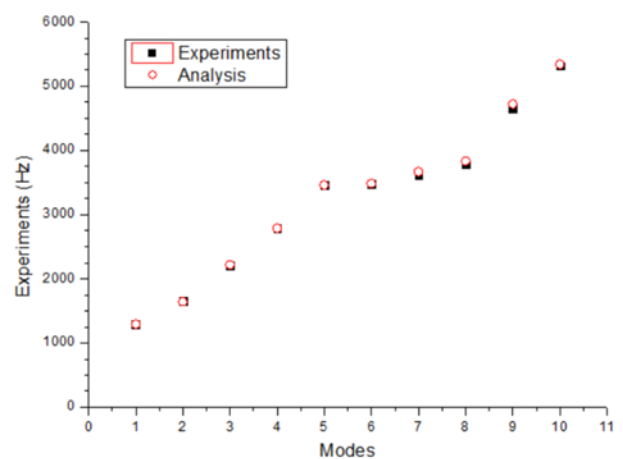


Fig. 4 Natural frequencies obtained from modal tests and finite element analysis of knuckle

squealing generation mechanism. To account for the stiffness of the car’s entire body frame by joining the surrounding parts, such as the shock absorber, lower control arm, steering gear, and others, spring

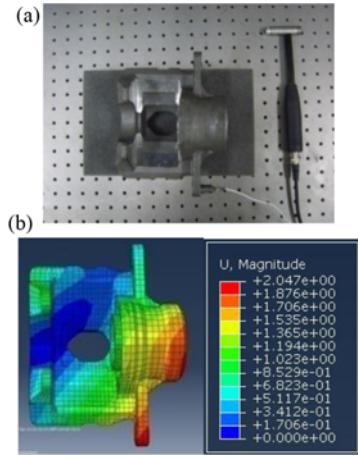


Fig. 5 Actual (a) and finite element housings (b) of caliper (legend: amplitude [mm])

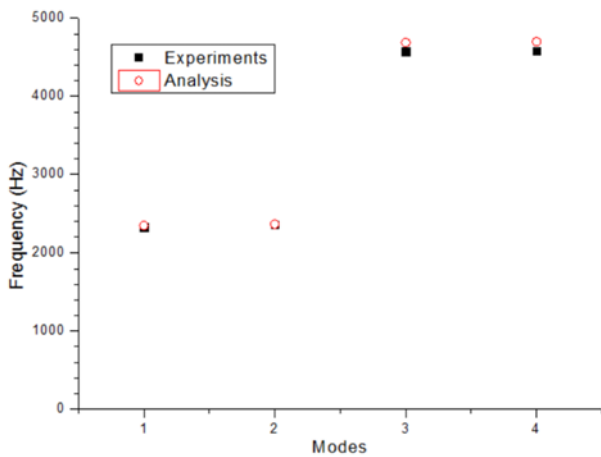


Fig. 6 Natural frequencies obtained from modal tests and finite element analysis of caliper

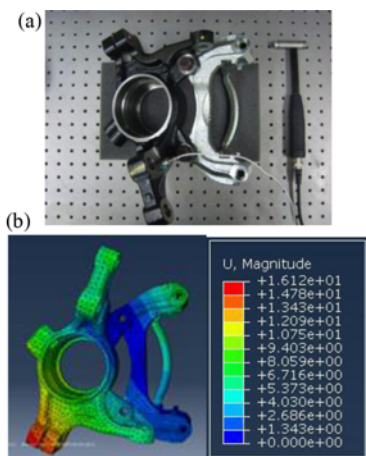


Fig. 7 Actual (a) and finite element assembly (b) consisting of carrier, knuckle, and housing (legend: amplitude [mm])

finite elements were used as shown in Fig. 8. The mechanical properties and 3-D finite elements that were used in the analysis of brake parts are listed in Table 1. The boundary conditions between two parts consisting

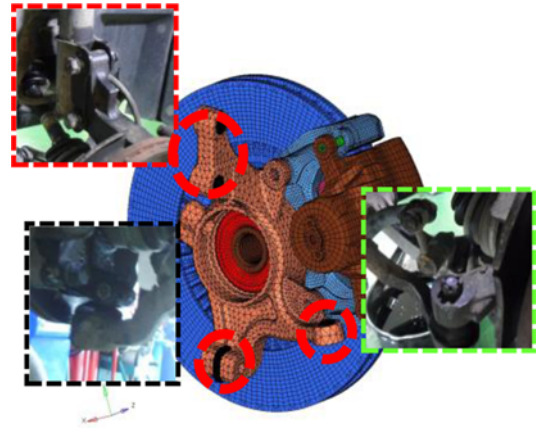


Fig. 8 Assembled finite element analysis model for brake system consisting of knuckle, disc, caliper, and carrier

Table 1 Mechanical properties and finite elements of brake parts

Parts	Density (kg/m <sup>3</sup> )	Young's Modulus (GPa)	Poisson's Ratio	Elements
Disc	7030	106	0.29	C3D6, C3D8
Knuckle	7430	178	0.29	C3D10
Piston	7820	210	0.29	C3D6, C3D8
Bearing	7820	210	0.29	C3D6, C3D8
Hub	7820	210	0.29	C3D6, C3D8
Pad spring	7820	210	0.29	C3D6, C3D8
Guide rod	7820	210	0.29	C3D6, C3D8
Pad	2477	0.32	0.00005	C3D6, C3D8
Pad lining	7677	221	0.29	C3D6, C3D8
Housing	7020	168	0.29	C3D6, C3D8
Carrier	7020	170	0.29	C3D6, C3D8

Table 2 Boundary conditions between two parts

B.C.'s	Between two parts
Fix	Guide Rod/Housing, Hub/Bearing, Carrier/Pad Spring
Contact	Bearing/Knuckle, Disc/Pad, Piston/Housing, Pad/Pad Spring

of the brake system were set to be fixed or contacted, depending on their relative motions, as demonstrated in Table 2.

### 3. Complex Eigenvalue Analysis

#### 3.1 Complex eigenvalue analysis

Complex eigenvalue analysis (CEA) is widely used to analyze brake squealing. The CEA calculates the complex valued eigenvalues of a brake system or component. The real part (*i.e.*, damping coefficient) indicates instability and the occurrence of brake squeal. The imaginary part of the complex eigenvalue is the damped natural frequency, and it is also responsible for the frequency of corresponding modes. A positive damping coefficient causes the amplitude of oscillations to increase with time. A complex eigenvalue method has been reported by Bajer et al. (2003),<sup>22</sup> and consists of four main processes as follows: (1) nonlinear static analysis to apply brake pressures; (2) nonlinear static analysis to impose an angular velocity on the disc; (3) normal mode

analysis to extract the natural frequency in order to constitute the projection subspace; (4) complex eigenvalue analysis to incorporate the effect of friction coupling.

The governing equation of a vibrating system can be generally expressed as:

$$[M]\{\ddot{u}\} + [C]\{\dot{u}\} + ([K_s] + \mu[K_f])\{u\} = \{0\} \quad (1)$$

where  $[M]$ ,  $[C]$ ,  $[K_s]$ ,  $[K_f]$ , and  $\mu$  are the mass matrix, damping matrix that includes friction-induced damping as well as material damping, structural stiffness matrix, asymmetrical friction induced stiffness matrix, and friction coefficient, respectively, while  $u$  is the displacement vector. Eq. (1) can be expressed in terms of the eigenvalue  $\lambda$  and corresponding eigenvector  $[\phi]$ .

The eigenvalues and eigenvectors in Eq. (2) may be complex and the equation should be symmetrized by ignoring the damping matrix  $[C]$  and the asymmetric stiffness matrix  $[K_f]$  in order to solve the complex eigenproblem. Alternatively, the symmetrized equation is solved in order to find the projected subspace. The  $N$  eigenvectors obtained from the symmetric eigenvalue problem are expressed as  $\{\phi_{sym}\}$ ; then, the original matrices are modified by projection onto the subspace of  $N$  eigenvectors, as shown in Eq. (3).

$$[\bar{M}] = \{\phi_{sym}\}^T [M] \{\phi_{sym}\} \quad (3a)$$

$$[\bar{C}] = \{\phi_{sym}\}^T [C] \{\phi_{sym}\} \quad (3b)$$

$$[\bar{K}] = \{\phi_{sym}\}^T ([K_s] + \mu[K_f]) \{\phi_{sym}\} \quad (3c)$$

By rearranging Eqs. (2) and (3), the projected complex eigenproblem is expressed as:

$$\{\lambda^2[\bar{M}] + \lambda[\bar{C}] + ([\bar{K}_s] + \mu[\bar{K}_f])\}\{\bar{\phi}\} = \{0\} \quad (4)$$

The approximation of the  $k$ -th complex eigenvectors  $\{\phi\}^k$  of the original system can be recovered from the projected eigenvector  $\{\bar{\phi}\}$ , as follows:

$$\{\phi\}^k = \{\phi_{sym}\}^T \{\bar{\phi}\}^k \quad (5)$$

Complex eigenvalue analysis was conducted to the current disc brake system under investigation. When the disc rotated at a constant tangential velocity of 3 km/h, a braking pressure of 0.5 MPa was applied to the piston in the caliper housing with the pad friction of 0.8, which considered the condition under which the squeal was likely to occur in an environment of high temperature and humidity. The constant damping coefficient of a lining material equal to 0.1 N·s/m was used in the following analyses. The natural frequencies were calculated by analysis with the FE model, and were observed up to the 100<sup>th</sup> mode, where the frequency was 5 kHz. Figs. 9-10 demonstrate the mode shapes at the natural frequencies of 3.544 and 3.981 kHz, which were obtained from this analysis.

The complex eigenvalue analysis was performed by using the natural frequencies obtained in the previous step, and the unstable modes at the specific frequencies were identified as shown in Fig. 11. The existing

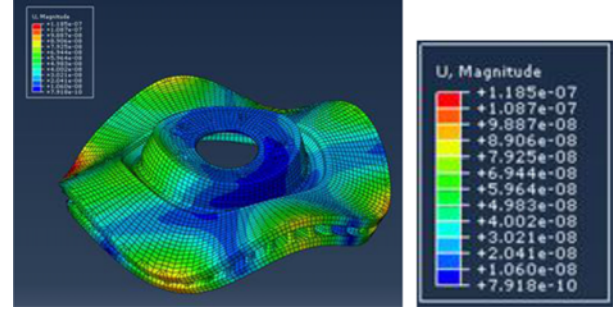


Fig. 9 Mode shape at the natural frequency of 3.544 kHz (legend: axial displacements [m])

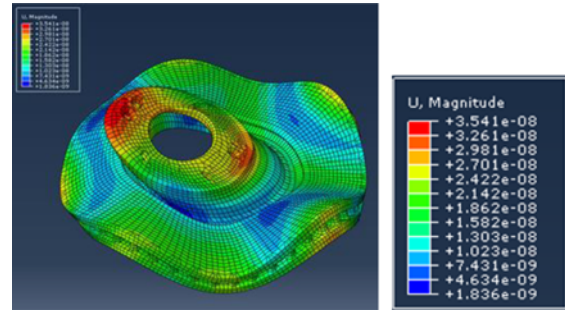


Fig. 10 Mode shape at the natural frequency of 3.981 kHz (legend: axial displacements [m])

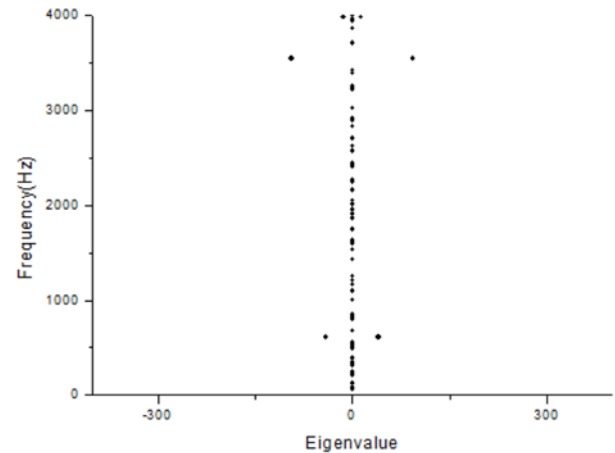


Fig. 11 Instabilities (*i.e.*, positive eigenvalues) computed by complex eigenvalue analysis of the current disc brake system

frequencies at positive eigenvalues mean that unstable modes occurred. The instabilities computed by CEA for the current disc brake system were observed at 3.544 kHz with an eigenvalue of 93.28, and an eigenvalue of 13.76 at 3.981 kHz, in the 3-kHz bandwidth of interest. An airborne noise called howling was also observed at 0.684 kHz, as shown in Fig. 11, which, however, did not qualify as squealing.

### 3.2 Contribution level to squeal

The concept of a component contribution factor (CCF) was proposed by (Zhang et al., 2003) in order to determine which brake component vibrates the most.<sup>31</sup> This concept is expressed by the following



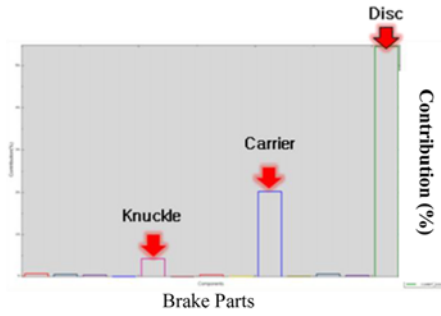


Fig. 12 Contribution percentage of each brake part to squealing at 3.544 kHz

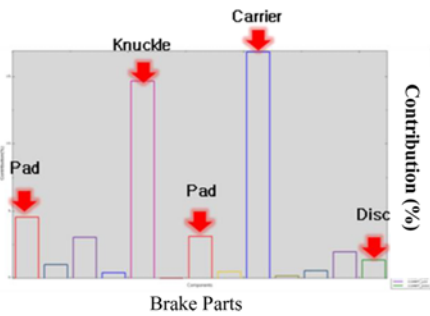


Fig. 13 Contribution percentage of each brake part to squealing at 3.981 kHz

equation:

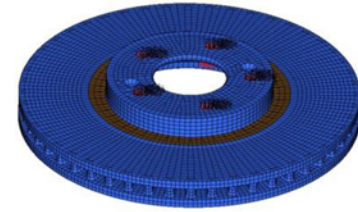
$$CCF = \frac{\{[\Phi_C^j]^T [W_V^C] [\Phi_C^j]\}^2}{\{[\Phi^j]^T [W_V] [\Phi^j]\}^2} \quad (6)$$

where  $\Phi_C^j$  and  $\Phi^j$  are the component and system mode shapes, respectively.  $W_V^C$  and  $W_V$  are the diagonal weighing matrices for the effective volume of each component  $C$  and the entire system, respectively, as follows:

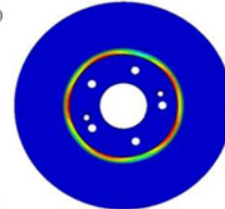
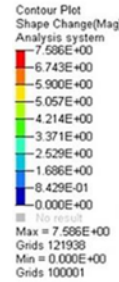
$$W_V^j = \sum_{j=1}^m \frac{V_j}{n} \quad (7)$$

where  $V$  is the volume of a component and  $n$  is the total element number of that component.

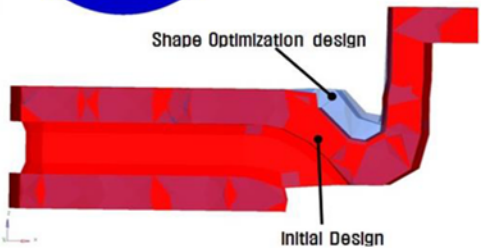
The squeal was predicted to occur at 3.544 kHz and 3.981 kHz in the 3 kHz bandwidth of interest by CEA, in order for the level of each part's contribution to the occurrence of squeal to be analyzed by FEM NVH analysis. The disc was the largest contributor to squealing, followed by the carrier and knuckle, which had the 2<sup>nd</sup> and the 3<sup>rd</sup> largest contribution, respectively, at 3.544 kHz. The two pads had insignificant contribution, as shown in Fig. 12. At 3.981 kHz, the carrier and knuckle contributed to squealing more than the disc, and even the two pads had a higher portion of squealing contribution in comparison to the disc, as shown in Fig. 13. In these two graphs, it was especially noticeable that the contribution of the knuckle was quite larger than what was expected before the analyses. The knuckle and its stiffness, which were usually omitted in most previous squeal analyses, must be included in the analyses for the prediction of disc brake squealing.



(a) Disc



Shape Optimization design



Initial Design

(b) Undercut shape (legend: shape changes [mm])

Fig. 14 Brake disc model and the optimal undercut around the disc hub

#### 4. Optimization and Dynamo Tests

The goal of this study was to suppress or remove the low-frequency squealing of the current disc brake system in the frequency of approximately 3 kHz. According to the CCF analysis, the disc had the largest squeal contribution at 3.544 kHz and, therefore, it was necessary to modify the current disc shape. Structural characteristics such as the number of vents, thicknesses of fin and disc, etc. impact disc squealing, which thus require an entirely new design with consideration to many mechanical principles. To achieve the goal with minimal design change, the groove shape around the disc hub and the carrier shape were targeted for modification in order to suppress the low-frequency squeal. In particular the influence of the carrier on squealing was the highest, as shown in Fig. 13.

The shape optimization of the groove was carried out using Optistruct.<sup>32,33</sup> The initial design domain is the current disc shape without the undercut near the hub, while the design variables are all the nodes in the shaded region around the hub, as shown in Fig. 14(a). The objective function was set in order to maximize the first natural frequency and thus remove the low-frequency squeal (1-3 kHz). With regard to constraints, the node directions were set to move in the direction of volume shrinkage. The optimum shape of an undercut is shown in Fig. 14(b). The size of the final undercut turns out to be smaller than the existing size, in order to increase disc stiffness. The optimal depth (11.6 mm) and width (15.4 mm) of the undercut shrunk by 35% relative to the current configuration. The natural frequencies of the disc in the optimal undercut shape increased by more than 20% in comparison to the existing undercut, which was not optimized, as

Table 3 Changes in natural frequencies after optimization of undercut

Modes	Natural frequency of the existing disc (Hz)	Natural frequency of the disc with an optimum undercut (Hz)
1st	603.1	747.1
2nd	835.6	1018.5
3rd	925.4	1110.4



Fig. 15 Newly manufactured brake disc with optimal undercut around the hub

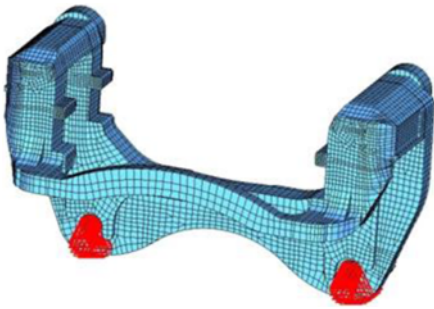


Fig. 16 FE model of a carrier in caliper disc brake

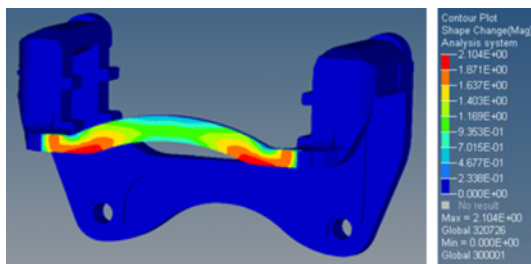


Fig. 17 Optimal carrier tie-bar shape (brightened part, legend: shape changes [mm])

summarized in Table 3. A small eigenvalue of 12.75 at 4.18 kHz was obtained from the complex eigenvalue analysis for the optimized undercut disc brake. A disc with optimal undercut around the hub was manufactured (Fig. 15).

The shape optimization of the carrier's tie-bar, which was an important part of the caliper, was performed. The initial middle width of the tie-bar was 10 mm. The cost function was set to maximize the 1<sup>st</sup> natural frequency. With regard to constraints, the node directions were set to move in the direction of the volume shrinkage. The design variables corresponded to all of the nodes in the tie-bar. The fixed boundary condition was applied to two holes, as shown in Fig. 16. As a result of shape optimization, the width of the middle of the tie-bar

increased to 11.5 mm, as shown in Fig. 17.

The modified brake disc with an optimal groove around the hub and the modified tie-bar in the caliper were newly designed and manufactured with a new mold, as shown in Fig. 15, in order to test whether the low-frequency squealing occurred or not. The brake dynamo test was carried out under the same conditions as those in the case of an actual car braking. The results of the squeal tests with the currently used disc at room temperature obtained the low-frequency squeal value of approximately 2.8 kHz (below 150 C). There was, however, no low-frequency squeal in the test of the modified disc with a smaller groove and caliper tie-bar at various velocities and pressures. Instead, a high frequency squeal occurred at 6.3 kHz only under the conditions of 3 km/h and 8 bars, and under a drag condition. From the dynamo test, it was observed that an optimal shape of the groove and tie-bar could effectively reduce the low-frequency squeal.

## 5. Conclusions

An accurate finite element model of a caliper brake, which consisted of a disc, knuckle, caliper, and parts (*i.e.*, housing, piston and oil seal, pads, pad springs, carrier, guide rod, etc.) was developed and each part was validated by modal tests. The unstable modes and the corresponding frequencies of the current brake were computed using CEA:

(1) The disc, carrier, and knuckle, in the order named, were found to be the major contributors to low-frequency squealing (at 3.544 kHz) by CCF analysis.

(2) As a result of cutting an optimal groove around the disc hub, CEA showed that the low-frequency squeal at 3,544 kHz did not occur, while a negligible level of squealing (negligible eigenvalue of 12.75) occurred at 4.18 kHz.

(3) The modified tie-bar and disc with optimal groove were manufactured by casting a new mold. In the disc brake dynamo experiments, a squeal was not measured at 3.544 kHz or 3.98 kHz.

It was proven that making an optimal groove around the disc hub and optimizing the tie-bar in the caliper were highly efficient in reducing the low-frequency squeal of the caliper brake.

## ACKNOWLEDGEMENT

This research was supported by the Kyungpook National University Research Fund, 2016.

## REFERENCES

1. Mechanical Engineering Publications Limited for the Institution, "Braking of Road Vehicles," 1976.
2. Guan, D. H. and Jiang, D. Y., "A Study on Disc Brake Squeal Using Finite Element Methods," SAE Technical Paper, No. 980597, 1998.
3. Kung, S.-W., Dunlap, K. B., and Ballinger, R. S., "Complex Eigenvalue Analysis for Reducing Low Frequency Brake Squeal," SAE Technical Paper, No. 2000-01-0444, 2000.

4. Nack, W. V., "Brake Squeal Analysis by Finite Elements," *International Journal of Vehicle Design*, Vol. 23, Nos. 3-4, pp. 263-275, 2000.
5. Shin, K., Brennan, M., Oh, J.-E., and Harris, C., "Analysis of Disc Brake Noise Using a Two-Degree-of-Freedom Model," *Journal of Sound and Vibration*, Vol. 254, No. 5, pp. 837-848, 2002.
6. Shin, K., Brennan, M. J., Oh, J.-E., and Harris, C. H., "Analysis of Disc Brake Noise using a Two-Degree-of-Freedom Model," *Journal of Sound and Vibration*, Vol. 254, No. 5, pp. 837-848, 2002.
7. Flint, J. and Hulten, J., "Lining-Deformation-Induced Modal Coupling as Squeal Generator in a Distributed Parameter Disc Brake Model," *Journal of Sound and Vibration*, Vol. 254, No. 1, pp. 1-21, 2002.
8. von Wagner, U., Hochlenert, D., and Hagedorn, P., "Minimal Models for Disk Brake Squeal," *Journal of Sound and Vibration*, Vol. 302, No. 3, pp. 527-539, 2007.
9. Lee, J.-M., Park, C., Chang, S., and Cho, S., "A Study on the Squeal Noise of Drum Brakes," *Journal of the Korean Society for Precision Engineering*, Vol. 15, No. 9, pp. 111-116, 1998.
10. Lee, C.-W., and Kim, J.-C., "Influence of the Speeds on the Curve Squeal Noise of Railway Vehicles," *Journal of the Korean Society for Precision Engineering*, Vol. 28, No. 5, pp. 572-577, 2011.
11. Jung, S. P., Park, T. W., Chai, J. B., and Chung, W. S., "Thermo-Mechanical Finite Element Analysis of Hot Judder Phenomenon of a Ventilated Disc Brake System," *International Journal of Precision Engineering and Manufacturing*, Vol. 12, No. 5, pp. 821-828, 2011.
12. Liles, G. D., "Analysis of Disc Brake Squeal Using Finite Element Methods," SAE Technical Paper, No. 891150, 1989.
13. Guan, D. and Huang, J., "The Method of Feed-In Energy on Disc Brake Squeal," *Journal of Sound and Vibration*, Vol. 261, No. 2, pp. 297-307, 2003.
14. Kang, J. Y., "Squeal Analysis of Gyroscopic Disc Brake System Based on Finite Element Method," *International Journal of Mechanical Sciences*, Vol. 51, No. 4, pp. 284-294, 2009.
15. Kang, J.-Y., "Mode Shape Variation of Disc Brake with Respect to Contact Stiffness Variation," *Transactions of the Korean Society of Automotive Engineers*, Vol. 18, No. 3, pp. 127-132, 2010.
16. Kang, J., Krousgrill, C. M., and Sadeghi, F., "Dynamic Instability of a Thin Circular Plate with Friction Interface and Its Application to Disc Brake Squeal," *Journal of Sound and Vibration*, Vol. 316, Nos. 1-5, pp. 164-179, 2008.
17. Kang, J., Krousgrill, C. M., and Sadeghi, F., "Comprehensive Stability Analysis of Disc Brake Vibrations Including Gyroscopic, Negative Friction Slope and Mode-Coupling Mechanisms," *Journal of Sound and Vibration*, Vol. 324, Nos. 1-2, pp. 387-407, 2009.
18. Kim, C. and Zhou, K., "Analysis of Automotive Disc Brake Squeal Considering Damping and Design Modifications for Pads and a Disc," *International Journal of Automotive Technology*, Vol. 17, No. 2, pp. 213-223, 2016.
19. Lee, H., "An Optimal Design Method for Brake Squeal Noise Based on Complex Eigenvalue and Sensitivity Analyses and Response Surface Methodology," Ph.D. Thesis, University of Michigan, Ann Arbor, 2000.
20. Mohammed, A. A. Y., and Rahim, I. A., "Analyzing the Disc Brake Squeal: Review and Summary," *International Journal of Scientific & Technology Research*, Vol. 2, No. 4, pp. 60-72, 2013.
21. Kinkaid, N., O'reilly, O., and Papadopoulos, P., "Automotive Disc Brake Squeal," *Journal of Sound and Vibration*, Vol. 267, No. 1, pp. 105-166, 2003.
22. Bajer, A., Belsky, V., and Zeng, L. J., "Combining a Nonlinear Static Analysis and Complex Eigenvalue Extraction in Brake Squeal Simulation," SAE Technical Paper, No. 2003-01-3349, 2003.
23. AbuBakar, A. R. and Ouyang, H., "Complex Eigenvalue Analysis and Dynamic Transient Analysis in Predicting Disc Brake Squeal," *International Journal of Vehicle Noise and Vibration*, Vol. 2, No. 2, pp. 143-155, 2006.
24. Liu, P., Zheng, H., Cai, C., Wang, Y. Y., Lu, C., et al., "Analysis of Disc Brake Squeal Using the Complex Eigenvalue Method," *Applied Acoustics*, Vol. 68, No. 6, pp. 603-615, 2007.
25. Junior, M. T., Gerges, S. N., and Jordan, R., "Analysis of Brake Squeal Noise Using the Finite Element Method: A Parametric Study," *Applied Acoustics*, Vol. 69, No. 2, pp. 147-162, 2008.
26. Dai, Y. and Lim, T. C., "Suppression of Brake Squeal Noise Applying Finite Element Brake and Pad Model Enhanced by Spectral-Based Assurance Criteria," *Applied Acoustics*, Vol. 69, No. 3, pp. 196-214, 2008.
27. Belhocine, A. and Bouchetara, M., "Thermo-Mechanical Coupled Analysis of Automotive Brake Disc," *International Journal of Precision Engineering and Manufacturing*, Vol. 14, No. 9, pp. 1591-1600, 2013.
28. Lee, H., "Vibro-Acoustic Characteristics of an Annular Disk with Narrow Radial Slots," *International Journal of Precision Engineering and Manufacturing*, Vol. 11, No. 5, pp. 689-696, 2010.
29. Yoo, C.-H., Park, J.-H., and Park, S.-S., "Design and Evaluation of Performance Tester for Yaw Brakes in Wind Turbines," *International Journal of Precision Engineering and Manufacturing-Green Technology*, Vol. 5, No. 1, pp. 81-87, 2018.
30. Kim, Y., Park, J., Lee, N.-K., and Yoon, J., "Profile Design of Loop-Type Blade for Small Wind Turbine," *International Journal of Precision Engineering and Manufacturing-Green Technology*, Vol. 4, No. 4, pp. 387-392, 2017.
31. Zhang, L., Wang, A., Mayer, M., and Blaschke, P., "Component Contribution and Eigenvalue Sensitivity Analysis for Brake Squeal," SAE Technical Paper, No. 2003-01-3346, 2003.
32. Jung, S. P., Kim, Y. G., and Park, T. W., "A Study on Thermal Characteristic Analysis and Shape Optimization of a Ventilated Disc," *International Journal of Precision Engineering and Manufacturing*,

Vol. 13, No. 1, pp. 57-63, 2012.

33. Nam, J.-H., Do, H.-C., and Kang, J.-Y., "Effect of Groove Surface on Friction Noise and Its Mechanism," *International Journal of Precision Engineering and Manufacturing*, Vol. 18, No. 8, pp. 1165-1172, 2017.